URSI GASS 2021, Rome, Italy, 28 August - 4 September 2021

Bessel beam scattering by a dielectric cylinder

Santi C. Pavone*(1), Gino Sorbello(1), and Loreto Di Donato(1)
(1) Department of Electrical, Electronics and Computer Engineering (DIEEI), University of Catania,
Viale Andrea Doria 6, 95125 Catania, Italy.

Abstract

The scattering of a Bessel beam (BB) incident field by a dielectric circular cylinder is here discussed and compared to more standard plane wave (PW) scattering, in such a way to clearly show that the scattering by BBs is more localized than that by PWs. Such an inherent localized scattering process, especially if applied to dense dielectric scatterers, offers new possibilities for imaging techniques at millimeter waves, especially of biological media.

1 Introduction

Diffractionless beams can be considered of great interest among researchers in electromagnetics, due to the possibility of using them for near-field beam collimation. Indeed, in several applications, such as in high-data rate transfer [1], imaging [2–4], ground penetrating radars (GPR) [5–7], and also for small particle manipulation [8], just to mention a few, the incident field is required to be highly localized, and diffraction has to be limited.

Among nondiffractive waves, Bessel beams (BBs) gained increasing importance since their introduction in optics [9], since they are able to focus energy in their main beam (that acts as a ray caustic), inside which the wavefront exhibits also the remarkable feature of being planar. This fact suggests the idea of using BBs as incident fields for scattering problems, thanks to their inherent beam localization.

In particular, if the scatterer is both a perfect electric conductor (PEC) and a dielectric, the BB inherently allows the scattering process to be spatially localized, since its main beam is dominantly involved in the scattering process, not the sidelobes, as a first approximation. Moreover, if the scatterer is a dense dielectric, i.e., when its dielectric permittivity is much greater than that of the surrounding medium, the scattering process is not so different from that by a PEC material under physical optics (PO) approximation [10]. In particular, most of the incident field is reflected back at the interface between the two media, since the intrinsic impedance jump at the interface is really high. On the other hand, the transmitted field strength is inherently weak, and directed along the local normal unit vector to the scatterer interface.

In order to prove the spatial localization of BB scattering process, in this paper it is compared with more standard PW scattering by a circular dielectric cylinder; indeed, it is shown that PW scattering produces in general a total electric field that inherently tends to wrap around the scattering surface, hence it cannot be considered spatially localized. To analyze the BB scattering, we consider the spectral representation of BBs in terms of PWs, thanks to the linearity of the problem at hand. The proposed results on BB scattering localization can support new applications of localized beams in scattering and microwave imaging such as, for instance, near-field radar cross section measurement (NF-RCS), GPR and through-the-wall linear imaging (TWI) [11–14]. For the sake of simplicity, we discuss a two dimensional (2D) transverse magnetic (with respect to the z-axis, TM^z) electromagnetic problem.

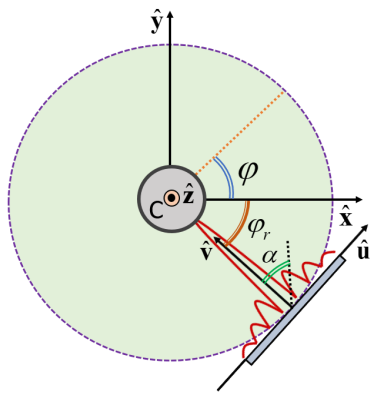

Figure 1. Bessel beam scattering by a dielectric circular cylinder: problem geometry definition, together with local and global reference systems.

The paper is structured as follows; in Section II, the formulation of BB scattering by a dielectric circular cylinder is briefly discussed, whereas in Section III, numerical results are shown to validate the theoretical model. Therefore, conclusions are drawn.

2 Problem analytical formulation

Let us consider the geometry of the 2D problem in Fig. 1, in which a dielectric circular cylindrical scatterer, oriented along the z-axis, is illuminated by a BB. For simplicity, the global Cartesian xy reference system is centered in correspondence of the cylinder axis, whereas the transmitting antenna is characterized by an auxiliary uv reference sys-

tem, in which $\hat{\mathbf{u}}$ unit vector is tangent to the circumference of radius R_m. We consider, without loss of generality, a TM^z illumination, so that $\mathbf{E}_{inc}^{BB} = E_{inc}^{BB}\hat{\mathbf{z}}$. The BB incident field can be written as superposition of PWs, that is

$$E_{inc}^{BB}(u,v) = \frac{1}{2\pi}\int_{-k}^{k}\gamma_{uv}(k_u)e^{-j\left(k_u u+\sqrt{k^2-k_u^2}v\right)}dk_u$$
$$= \frac{k}{2\pi}\int_{-\pi/2}^{\pi/2}\gamma_{uv}(\alpha)e^{-jk(\sin\alpha u+\cos\alpha v)}\cos\alpha d\alpha, \quad (1)$$

in which

$$\gamma_{uv}(\alpha) = \int_{-\infty}^{+\infty}J_0(k_{ua}u')\Pi\left(\frac{u'}{L}\right)e^{jk\sin\alpha u'}du', \quad (2)$$

being $k_u = k\sin\alpha$, $k_{ua} = k\sin\alpha_a$ the imposed wavenumber on the linear source, $H_0^{(1,2)}(\cdot)$ the zeroth order, first (second) kind Hankel function, L the transmitting antenna length, k and η the free-space wavenumber and intrinsic impedance, respectively, α_a the so-called axicon angle [7, 9].
In (2), a truncated cylindrical standing wave distribution (CSW) $J_0(k_{ua}u')\Pi(u'/L)$ has been imposed to radiate a BB generation in free-space. Indeed, it is well-established in literature [7, 15] that such a distribution is able to radiate a nondiffractive Bessel beam up to a finite distance called nondiffractive range [7, 9].
To evaluate quantitatively the BB incident field localization in the scattering problem, the half-power beamwidth normalized to the wavelength (HPBW$_\lambda$) is introduced, defined as

$$\text{HPBW}_\lambda = \frac{\text{HPBW}}{\lambda} = \frac{0.48}{\sin\alpha_a}, \quad (3)$$

in which $\lambda = 2\pi/k$ is the operating wavelength.
It is worth noting that the complex spectral weights $\gamma_{uv}(\alpha)$ used for BB reconstruction by PW elementary contributions are referred to the local uv reference system, thus to refer them to the global reference system xy normally adopted for scattering description, an angle-dependent phase compensation is required, namely

$$\gamma_{xy}(\alpha,\phi,\phi_r) = \gamma_{uv}(\alpha)e^{-jk\cos(\phi-\phi_r)R_a}, \quad (4)$$

being $R_a = \sqrt{(x-x_a)^2+(y-y_a)^2}$, whereas (x_a, y_a) are the coordinates of the feeding array center, and ϕ_r the azimuthal orientation of the array with respect to the global xy frame, as shown in Fig. 1.
The scattered field due to BB incident field by a dielectric cylinder, placed at the center of the global xy reference system, is then considered. For simplicity, we denote by $\rho = \rho\cos\phi\hat{\mathbf{x}} + \rho\sin\phi\hat{\mathbf{y}}$ the observation point. The constituent PW contribution is assumed to be of unitary amplitude and phasing $e^{-jk\rho\cos(\phi-\phi_r)}$, wherein ϕ_r denotes the incidence angle (Fig. 1). The PW scattered field $\mathbf{E}_{sct}^{PW} = E_{sct}^{PW}\hat{\mathbf{z}}$ by a dielectric cylinder can be expressed through the cylindrical wave expansion, i.e.,

$$E_{sct}^{PW}(\rho) = \sum_{-\infty}^{+\infty}a_n H_n^{(2)}(k\rho)e^{jn(\phi-\phi_r)}, \quad (5)$$

in which

$$a_n = j^{-n}\frac{\eta_0 J_n'(kr_c)J_n(k_d r_c) - \eta_d J_n(kr_c)J_n'(k_d r_c)}{\eta_d J_n'(k_d r_c)H_n^{(2)}(kr_c) - \eta_0 J_n(k_d r_c)H_n'^{(2)}(kr_c)}, \quad (6)$$

being r_c the scatterer radius, $J_n'(\cdot)$ and $H_n'^{(2)}(\cdot)$ the derivatives of Bessel and Hankel functions with respect to their arguments, whereas $\eta_0 = \sqrt{\varepsilon_0/\mu_0} \approx 377\Omega$ is the free-space impedance, and $\eta_d = \eta_0\sqrt{\varepsilon_r/\mu_r}$ is instead the intrinsic impedance of the medium of which the scatterer is made. Furthermore, to determine the scattered field under BB illumination, i.e., $\mathbf{E}_{sct}^{BB} = E_{sct}^{BB}\hat{\mathbf{z}}$, we exploit the angular spectrum coefficients given by (4), so that

$$E_{sct}^{BB}(\rho) = \frac{k}{2\pi}\int_{-\pi/2}^{\pi/2}\gamma_{xy}(\phi_r)E_{sct}^{PW}(\rho,\phi_r)\cos\phi_r d\phi_r, \quad (7)$$

which represents the scattered field by a BB impinging orthogonally with respect to the local tangent plane to the scatterer PEC surface. Following the above explained procedure, the scattering problem can be handled as a continuous superposition of scattered PW fields, weighted by the relevant Fourier coefficients. Such an expression is easy to be implemented and gives an exact solution to the problem at hand. The total electric field, $\mathbf{E}_{tot}^{BB,PW} = E_{tot}^{BB,PW}\hat{\mathbf{z}}$, due to both PW and BB incident fields, can be finally calculated as the sum of incident and scattered fields [16], namely

$$E_{tot}^{BB,PW}(\rho) = E_{inc}^{BB,PW}(\rho) + E_{sct}^{BB,PW}(\rho). \quad (8)$$

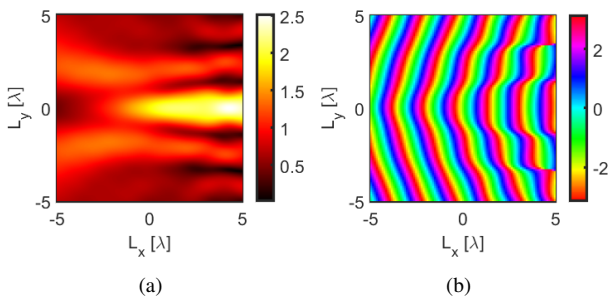

Figure 2. (a) Amplitude and (b) phase of BB incident field, by considering the following parameters: axicon angle $\alpha_a = 25°$, abscissa of the radiating array $L_x = 6\lambda$, length of the radiating array: $L = 12\lambda$.

3 Numerical examples

In this Section, the scattering of a PW and a BB by a dielectric circular cylinder is numerically analyzed and discussed, in the particular case of dense scatterer, i.e., for which the dielectric permittivity is much greater than that of the background medium. Such a case is of interest, for instance, for biological imaging, since it is well-known that biological media usually exhibit an high electrical permittivity.
Without loss of generality, in the following we will consider

a BB characterized by an axicon angle $\alpha_a = 25°$ [7, 9], radiated by a current distribution of length $L = 12\lambda$, parallel to the y-axis, and placed at a distance $L_x = 6\lambda$ from the center of the global xy reference system. In Fig. 2, the BB incident field is shown (a) in amplitude and (b) phase. As it is apparent, inside its main lobe the wavefront is locally planar, and this fact is really of interest for imaging purposes. Moreover, the main lobe acts as a ray caustic for the beam [7, 17], hence most of the energy can be localized inside it.

As a numerical example, in Fig. 3 we show and compare

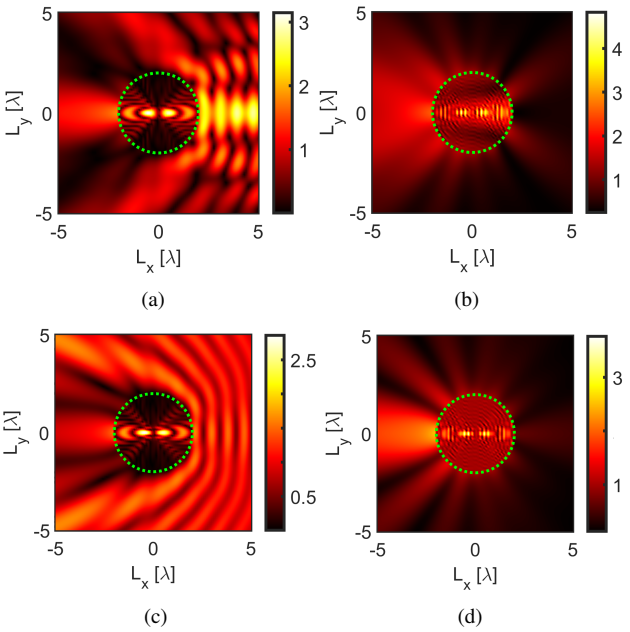

Figure 3. Scattering of both BB and PW by a dense dielectric circular cylinder ($\varepsilon_r = 81$) of radius equal to 2λ. (a) Amplitude of BB total electric field. (b) Amplitude of BB scattered electric field. (c) Amplitude of PW total electric field. (d) Amplitude of PW scattered electric field.

the scattering of a BB with that of a standard PW by a dense dielectric circular cylinder of radius $r_c = 2\lambda$, placed at the center of the global xy reference system, whose electric relative permittivity is $\varepsilon_r = 81$, corresponding to a refractive index $n = 9$. In particular, in Fig. 3(a)-(c) the total electric fields E_{tot}^{BB} and E_{tot}^{PW} are shown, respectively, whereas in Fig. 3(b)-(d) the scattered electric fields E_{sct}^{BB} and E_{sct}^{PW} are presented. As it is apparent especially from the color maps associated to total electric fields, the BB scattering is effectively a more localized phenomenon than that from a PW; indeed, a stationary wave arises in the backward region, i.e., for $L_x > 0$ and $L_y \in (-\infty, +\infty)$, due to the presence of a wave reflected back from the localized scattering region at the interface between the background medium and the dense dielectric. Conversely, the PW incident field inherently wraps around the scatterer, hence the scattering process is not localized; then, similarly, the total electric field E_{tot}^{PW} shows a diffused stationary pattern, due to the non local scattering process.

Similar results can be obtained also by considering the case of less dense dielectrics, as it can be inferred from Fig. 4, in which the scattering of both BB and PW incident fields by a dielectric circular cylinder of radius $r_c = 1\lambda$ and relative electrical permittivity $\varepsilon_r = 40$ is shown. The interesting

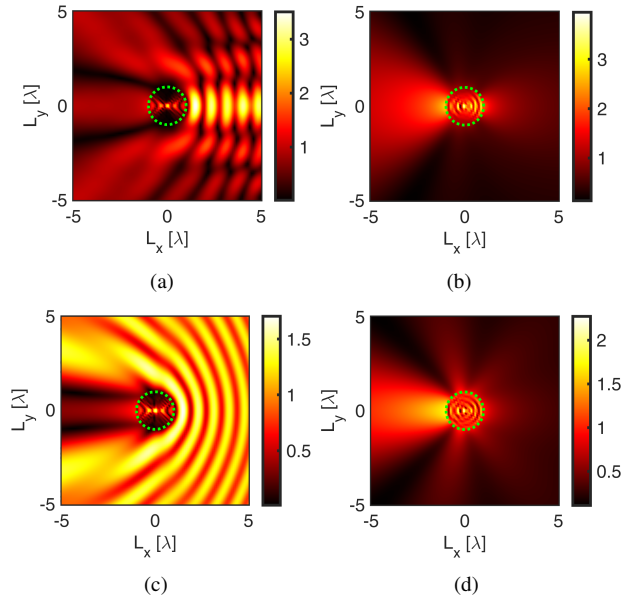

Figure 4. Scattering of both BB and PW by a dielectric circular cylinder ($\varepsilon_r = 40$) of radius equal to 1λ. (a) Amplitude of BB total electric field. (b) Amplitude of BB scattered electric field. (c) Amplitude of PW total electric field. (d) Amplitude of PW scattered electric field.

and inherent localization of BB incident fields with respect to PW counterpart, both for PEC and dense dielectric scatterers, opens new and interesting possibilities to apply BBs and in general nondiffractive waves in imaging problems at microwaves/millimeter waves.

4 Conclusions

In this paper, we proposed the scattering analysis of Bessel beams by a dielectric circular cylinder, and we compared it to more classical plane wave scattering under same conditions. We have shown that Bessel beams, due to their inherent focused nature, provide localized scattering phenomenon, differently from plane wave counterparts. To conclude, this result paves the way to new effective applications of nondiffractive waves for imaging purposes.

Acknowledgements

Santi C. Pavone would like to thank the project PON-AIM "Attraction and International Mobility", granted by the Italian Ministry of University and Scientific Research (MUR).

References

[1] S. Chen, S. Li, Y. Zhao, J. Liu, L. Zhu, A. Wang, J. Du, L. Shen, and J. Wang, "Demonstration of 20-gbit/s high-speed bessel beam encoding/decoding link with adaptive turbulence compensation," *Opt. Lett.*, vol. 41, no. 20, pp. 4680–4683, 2016.

[2] J. Lu and J. F. Greenleaf, "Ultrasonic nondiffracting transducer for medical imaging," *IEEE Trans. ultrason. ferroelectr. freq. contr.*, vol. 37, no. 5, pp. 438–447, 1990.

[3] K.-S. Lee and J. P. Rolland, "Bessel beam spectral-domain high-resolution optical coherence tomography with micro-optic axicon providing extended focusing range," *Opt. Lett.*, vol. 33, no. 15, pp. 1696–1698, 2008.

[4] T. A. Planchon, L. Gao, D. E. Milkie, M. W. Davidson, J. A. Galbraith, C. G. Galbraith, and E. Betzig, "Rapid three-dimensional isotropic imaging of living cells using Bessel beam plane illumination," *Nat. meth.*, vol. 8, no. 5, pp. 417–423, 2011.

[5] D. Mugnai and P. Spalla, "Electromagnetic propagation of Bessel-like localized waves in the presence of absorbing media," *Opt. Comm.*, vol. 282, no. 24, pp. 4668–4671, 2009.

[6] A. Mazzinghi, M. Balma, D. Devona, G. Guarnieri, G. Mauriello, M. Albani, and A. Freni, "Large depth of field pseudo-Bessel beam generation with a rlsa antenna," *IEEE Trans. Antennas Propag.*, vol. 62, no. 8, pp. 3911–3919, 2014.

[7] M. Ettorre, S. C. Pavone, M. Casaletti, M. Albani, A. Mazzinghi, and A. Freni, "Near-field focusing by non-diffracting Bessel beams," in *Aperture Antennas for Millimeter and Sub-Millimeter Wave Applications*. Springer, 2018, pp. 243–288.

[8] J. Arlt, V. Garcés-Chávez, W. Sibbett, and K. Dholakia, "Optical micromanipulation using a bessel light beam," *Opt. Comm.*, vol. 197, no. 4-6, pp. 239–245, 2001.

[9] J. Durnin, "Exact solutions for nondiffracting beams. I. The scalar theory," *JOSA A*, vol. 4, no. 4, pp. 651–654, 1987.

[10] A. J. Devaney, *Mathematical foundations of imaging, tomography and wavefield inversion*. Cambridge University Press, 2012.

[11] H.-T. Chou, W.-J. Gao, J.-H. Zhou, B.-Q. You, and X.-H. He, "Enhancing electromagnetic backscattering responses for target detection in near zone of near-field focused phased array antennas," *IEEE Trans. Antennas Propag.*, 2020.

[12] M. Bevacqua, L. Crocco, L. D. Donato, T. Isernia, and R. Palmeri, "Exploiting sparsity and field conditioning in subsurface microwave imaging of nonweak buried targets," *Radio Science*, vol. 51, no. 4, pp. 301–310, 2016.

[13] L. Di Donato, R. Palmeri, G. Sorbello, T. Isernia, and L. Crocco, "A new linear distorted-wave inversion method for microwave imaging via virtual experiments," *IEEE Trans. Microw. Theory Techn.*, vol. 64, no. 8, pp. 2478–2488, 2016.

[14] S. C. Pavone, G. Sorbello, and L. Di Donato, "On the orbital angular momentum incident fields in linearized microwave imaging," *Sensors*, vol. 20, no. 7, p. 1905, 2020.

[15] S. C. Pavone, A. Mazzinghi, A. Freni, and M. Albani, "Comparison between broadband bessel beam launchers based on either Bessel or Hankel aperture distribution for millimeter wave short pulse generation," *Opt. Expr.*, vol. 25, no. 16, pp. 19 548–19 560, 2017.

[16] C. A. Balanis, *Advanced engineering electromagnetics*. John Wiley & Sons, 2012.

[17] S. C. Pavone, M. Ettorre, M. Casaletti, and M. Albani, "Analysis and design of Bessel beam launchers: Transverse polarization," *IEEE Trans. Antennas Propag. (to appear)*, 2021.